Excitation-Energy Migration in Self-Assembled Cyclic Zinc(II)-Porphyrin Arrays: A Close Mimicry of a Natural Light-Harvesting System

ARTICLE *in* CHEMISTRY · JUNE 2005

Impact Factor: 5.73 · DOI: 10.1002/chem.200500069 · Source: PubMed

16 AUTHORS, INCLUDING:

Dongho Kim
Yonsei University
496 PUBLICATIONS **13,337** CITATIONS
SEE PROFILE

Fuyuki Ito
Shinshu University
39 PUBLICATIONS **393** CITATIONS
SEE PROFILE

Yutaka Nagasawa
Ritsumeikan University
82 PUBLICATIONS **2,391** CITATIONS
SEE PROFILE

Hiroshi Miyasaka
Osaka University
211 PUBLICATIONS **4,147** CITATIONS
SEE PROFILE

Excitation-Energy Migration in Self-Assembled Cyclic Zinc(II)–Porphyrin Arrays: A Close Mimicry of a Natural Light-Harvesting System

In-Wook Hwang,[a] Mira Park,[a] Tae Kyu Ahn,[a] Zin Seok Yoon,[a] Dah Mee Ko,[a] Dongho Kim,*[a] Fuyuki Ito,[b] Yukihide Ishibashi,[b] Sazzadur R. Khan,[b] Yutaka Nagasawa,[b] Hiroshi Miyasaka,*[b] Chusaku Ikeda,[c] Ryoichi Takahashi,[c] Kazuya Ogawa,[c] Akiharu Satake,[c] and Yoshiaki Kobuke*[c]

Abstract: The excitation-energy-hopping (EEH) times within two-dimensional cyclic zinc(II)–porphyrin arrays **5** and **6**, which were prepared by intermolecular coordination and ring-closing metathesis reaction of olefins, were deduced by modeling the EEH process based on the anisotropy depolarization as well as the exciton–exciton annihilation dynamics. Assuming the number of energy-hopping sites $N=5$ and 6, the two different experimental observables, that is, anisotropy depolarization and exciton–excition annihilation times, consistently give the EEH times of 8.0 ± 0.5 and 5.3 ± 0.6 ps through the 1,3-phenylene linkages of **5** and **6**, respectively. Accordingly, the self-assembled cyclic porphyrin arrays have proven to be well-defined two-dimensional models for natural light-harvesting complexes.

Keywords: energy transfer · femtosecond transient absorption · fluorescence spectroscopy · polarization anisotropy · porphyrinoids

Introduction

There have been numerous studies on the syntheses of covalently linked porphyrin arrays with a variety of linkers; these investigations inevitably require elaborate and time-consuming work.[1–8] The overall structures of porphyrin arrays hitherto prepared, however, are still remote from those of natural light-harvesting systems, mainly due to a lack of fine control of synthetic capabilities. As a supplementary route, a synthetic strategy that utilizes supramolecular chemistry has been envisaged, because it provides versatility in molecular networking in multidimensional space to increase the efficiency in light harvesting and electronic communication.[9–15] In this way, it becomes possible to prepare self-assembled porphyrin arrays in circular arrangements,[10d,e] which are closer mimics of light-harvesting complexes 1 and 2 (LH1 and LH2) in nature.[16]

In this context, we have developed cyclic porphyrin arrays in which five or six slipped cofacial zinc(II)–diporphyrin complexes, constructed by the complementary coordination of imidazolyl to zinc with a stability constant of the order of $10^{11}\,\text{M}^{-1}$, are connected together through 1,3-phenylene linkages (Scheme 1). In a previous communication, we reported the formation of self-assembled cyclic hexamer and pentamer of an imidazolyl-substituted gable porphyrin.[10d] To fur-

[a] Dr. I.-W. Hwang, M. Park, T. K. Ahn, Z. S. Yoon, D. M. Ko, Prof. D. Kim
Center for Ultrafast Optical Characteristics Control and Department of Chemistry, Yonsei University
Seoul 120–749 (Korea)
Fax: (+82) 2-2123-2434
E-mail: dongho@yonsei.ac.kr

[b] F. Ito, Y. Ishibashi, Dr. S. R. Khan, Prof. Y. Nagasawa, Prof. H. Miyasaka
Division of Frontier Materials Science
Graduate School of Engineering Science and Research Center of Materials Science at Extreme Conditions
Osaka University, Toyonaka, Osaka 560–8531 (Japan)
Fax: (+81) 6-6850-6244
E-mail: miyasaka@chem.es.osaka-u.ac.jp

[c] C. Ikeda, R. Takahashi, K. Ogawa, A. Satake, Prof. Y. Kobuke
Graduate School of Materials Science
Nara Institute of Science and Technology
Takayama 8916–5, Ikoma, Nara 630–0101 (Japan)
Fax: (+81) 7-4372-6119
E-mail: kobuke@ms.aist-nara.ac.jp

Supporting information for this article is available on the WWW under http://www.chemeurj.org/ or from the author. It contains data for the rotational diffusion time in solution, and EEH dynamics of **3**.

 DOI: 10.1002/chem.200500069

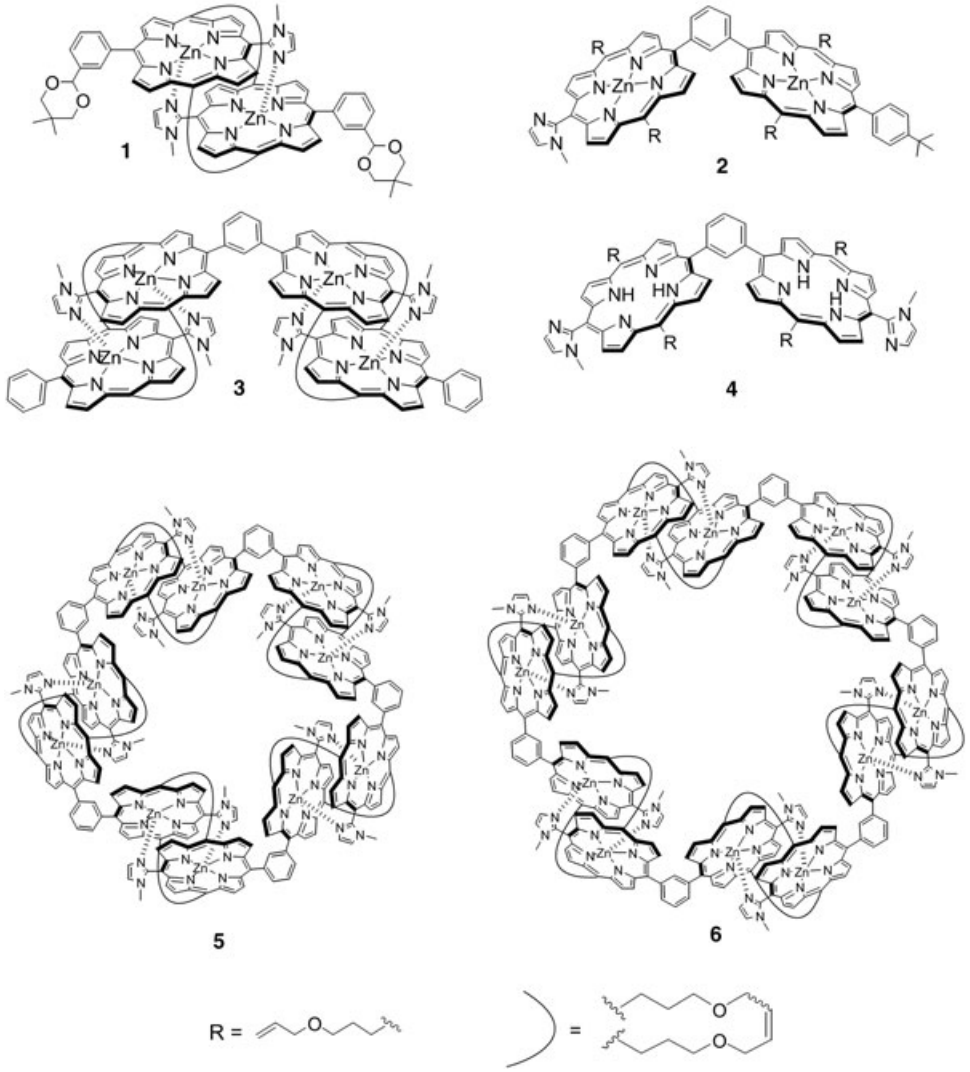

Scheme 1. Molecular structures of cofacially linked zinc(II)–diporphyrin **1**, 1,3-phenylene-linked zinc(II)–diporphyrin **2**, 1,3-phenylene-linked zinc(II)–tetraporphyrin **3**, 1,3-phenylene-linked freebase diporphyrin **4**, and 1,3-phenylene-linked cyclic zinc(II)–pophyrin arrays **5** and **6**.

ther increase the stability, the macrocycles were covalently fixed by olefin metathesis reactions of the coordination pairs affording the detection of molecular-ion peaks corresponding to 5-mer **5** and 6-mer **6** in MALDI-TOF mass measurements (Scheme 1).[17] The fixation is further expected to be useful for the photophysical measurements without scrambling even in coordinating solvent such as pyridine,[9] which generally dissociates the coordination to reduce the macrocycles into the monomeric units. Besides the circular arrangement, complexes **5** and **6** are especially well suited as models for LH1 and B850 in the LH2, because the close slipped cofacial dimeric arrangements along with regular separations are similar to the overall structures.[16–18]

As a model for LH1 and LH2 complexes, it is indispensable to understand interchromophoric interactions, such as exciton coupling and energy migration processes.[6g, 9b,9c] To reveal the excitation-energy-hopping (EEH) phenomena occurring in **5** and **6**, the polarization changes between the ground and excited states have been examined by means of fluorescence anisotropy and femtosecond transient absorption anisotropy (TAA). While the nanosecond time-resolved fluorescence anisotropy provides relevant information on the rotational diffusion motion of molecules in solution, femtosecond TAA measurements give direct evidence about the EEH, because the initial localization of the excitations in weakly coupled multichromophores gives rise to a rapid change in depolarization as the excitation energy is transferred. The observed exciton–exciton annihilation process is also associated with the EEH, because this process can be considered as an incoherent energy-hopping process from the excited donor to the proximal excited acceptor.[6g, 9c] Based on both anisotropy depolarization and exciton–exciton annihilation processes, we were able to quantify the EEH times for the cyclic arrays **5** and **6**.

Results

Construction of cyclic porphyrin arrays 5 and 6: The synthetic procedures for the preparation of the samples were previously reported.[17] The imidazolyl-substituted gable porphyrin **4** with allyloxypropyl substituents at the *meso*-positions was synthesized from 5-(3-formylphenyl)-15-imidazolylporphyrin, which was synthesized by the reaction of *N*-methylimidazole-2-carbaldehyde (1 equiv), allyloxypropyldipyrromethane (2 equiv), and monoprotected isophtalaldehyde (1 equiv) with CF_3CO_2H (TFA, 3 equiv) followed by chloranil oxidation. The isolation was performed by SiO_2 column chromatography and recycling GPC-HPLC to afford pure freebase **4** in 17% yield. GPC analysis of the mixture obtained after zinc insertion showed a broad molecular weight distribution. The self-assembled arrays were dissociated to smaller oligomers by dissolving in $CHCl_3$/methanol [first in 5 μM of $CHCl_3$/methanol = 7:3 (v/v) and then further diluted by adding methanol to make a 3.5 μM solution of $CHCl_3$/methanol = 1:1 (v/v)], and then the solvent was evaporated slowly at 25 ± 1 °C.

This reorganization process under high dilution conditions allowed the selective formation of 5-mer and 6-mer. After reorganization the mixture was subjected to the metathesis reaction by Grubbs catalyst to afford covalently linked cyclic 5-mer **5** and 6-mer **6** as evidenced by MALDI-TOF mass measurements. Scheme 1 illustrates the structures of these compounds along with reference porphyrins employed in our measurements.

Steady-state absorption, fluorescence, and fluorescence excitation anisotropy: Figure 1 shows the absorption and fluorescence spectra of two reference zinc(II)–diporphyrins (**1**, **2**) and the two cyclic zinc(II)–porphyrin arrays **5** and **6**; to prevent self assembly complex **2** was dissolved in pyridine[9] to give pyridine-coordinated **2**, whereas the others complexes were dissolved in toluene. The peak positions are summarized in Table 1. The absorption spectra of **5** and **6** are characteristic of cofacially self-assembled zinc(II)–diporphyrin **1**, exhibiting the Soret bands (S_0–S_2) that are split due to excitonic dipole–dipole coupling[10d,17,19] between zinc(II)–porphyrin monomers. In **5** and **6**, the splitting in the Soret bands is larger than that of **1** and a new band appears at 425 nm, indicating additional dipole couplings between units of **1** through the 1,3-phenylene linkage, as also seen in the splitting in the Soret bands of **2** and **3** (see the Supporting Information). These exciton couplings consequently indicate Förster-type incoherent energy-hopping processes within and between units of **1**. The splitting of **6** (2119 cm^{-1}) is slightly larger than that of **5** (2019 cm^{-1}), indicating relatively larger exciton interactions in the case of **6**. The Soret bands of **5** and **6** show negligible differences on changing the solvent, implying that pyridine cannot disturb the robust cyclic structures of **5** and **6**, which are formed by zinc(II)–imidazole coordination and the ring-closing metathesis reaction with an olefinic alkyl chain (Figure 1, inset). The fluorescence spectra of **5** and **6** exhibit two peaks at 627 and 682 nm, which are also similar to those found for **1**. Thus the absorption and fluorescence spectra of **5** and **6** are mainly determined by electronic interaction between two zinc(II)–porphyrin monomers within the units of **1**.

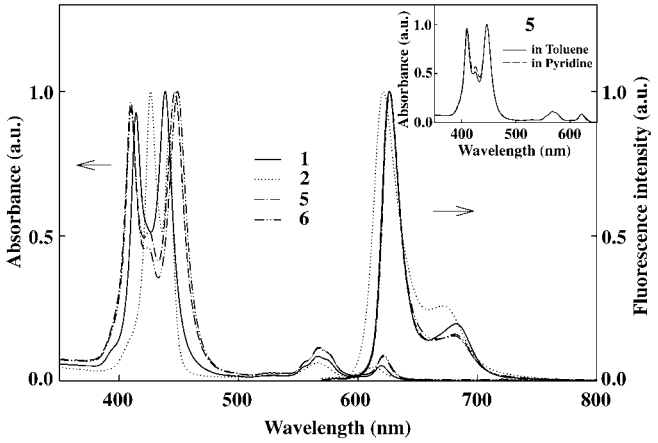

Figure 1. Steady-state absorption and fluorescence spectra of **1**, **2**, **5**, and **6** recorded in toluene except for **2**, which was recorded in pyridine. Inset compares the absorption spectra of **5** measured in toluene and pyridine. The fluorescence spectra were obtained with the 410 nm excitation, for which the excitation wavelength dependence was negligible.

The steady-state fluorescence excitation anisotropy spectra monitored at 625 nm are displayed for complexes **1** and **2**, and arrrays **5** and **6** (Figure 2). The fluorescence excitation anisotropy measurement gives information about the angle difference between absorption and emission dipoles as well as the EEH process.[9c,19] Complexes **1** and **2** display the profiles exhibiting slightly negative anisotropy in the high-energy Soret band and positive anisotropies in the low-energy Soret and Q bands. The negative anisotropy in the high-energy Soret band indicates EEH process occurring between zinc(II)–porphyrin monomers of **1** and **2**, with respect to the positive anisotropy[20] in the entire Soret band of zinc(II)–porphyrin monomer. Arrays **5** and **6** exhibit larger negative anisotropies in the high-energy Soret band and smaller positive anisotropies in the low-energy Soret and Q bands, accordingly indicating efficient EEHs within and between units of **1**. The excitation energy transfer between the same molecular units with different orientations generally gives rise to smaller fluorescence excitation anisotropy, resulting in new depolarization channels.[9c]

Fluorescence lifetime and fluorescence anisotropy decay: The time-resolved fluorescence decays of **1**, **2**, **5**, and **6** were measured (see the Supporting Information), and their fitted fluorescence lifetimes are listed in Table 2. The fluorescence decay profiles exhibit single exponential decays, and their lifetimes are all similar, except for a slightly shorter fluorescence lifetime for **2**. These results indicate that the excited S_1 states are also governed by the electronic state formed by the cofacial interactions within units of **1**. In addition, the long S_1 state lifetimes reflect an avoidance of energy-sinks in **5** and **6**, which is an important requirement in the EEH process.

The fluorescence anisotropy decay profiles of **1**, **2**, **5**, and **6** were also measured (see the Supporting Information), for which the excitation of the high-energy Soret band, that is, $\lambda_{ex}=410$ nm, was employed. The fitted decay parameters are listed again in Table 2. The

Table 1. Band maxima in absorption and fluorescence spectra of samples **1**, **2**, **5**, and **6**.[a]

	Absorption [nm]				Fluorescence [nm][c]	
	Soret (high)[b]	Soret (low)	Q(1,0)	Q(0,0)	Q(0,0)	Q(0,1)
1	414	439	554, 566, 574	619	626	684
2	426	442	567	613	621	672
5	410(s), 425(w)	447	555, 567, 575	621	626.5	682
6	410(s), 425(w)	449	555, 567, 575	622	627	682

[a] The solvents used were pyridine for **2** and toluene for the others. [b] The nomenclature s and w in parentheses indicates strong and weak. [c] An excitation wavelength of 410 nm was used.

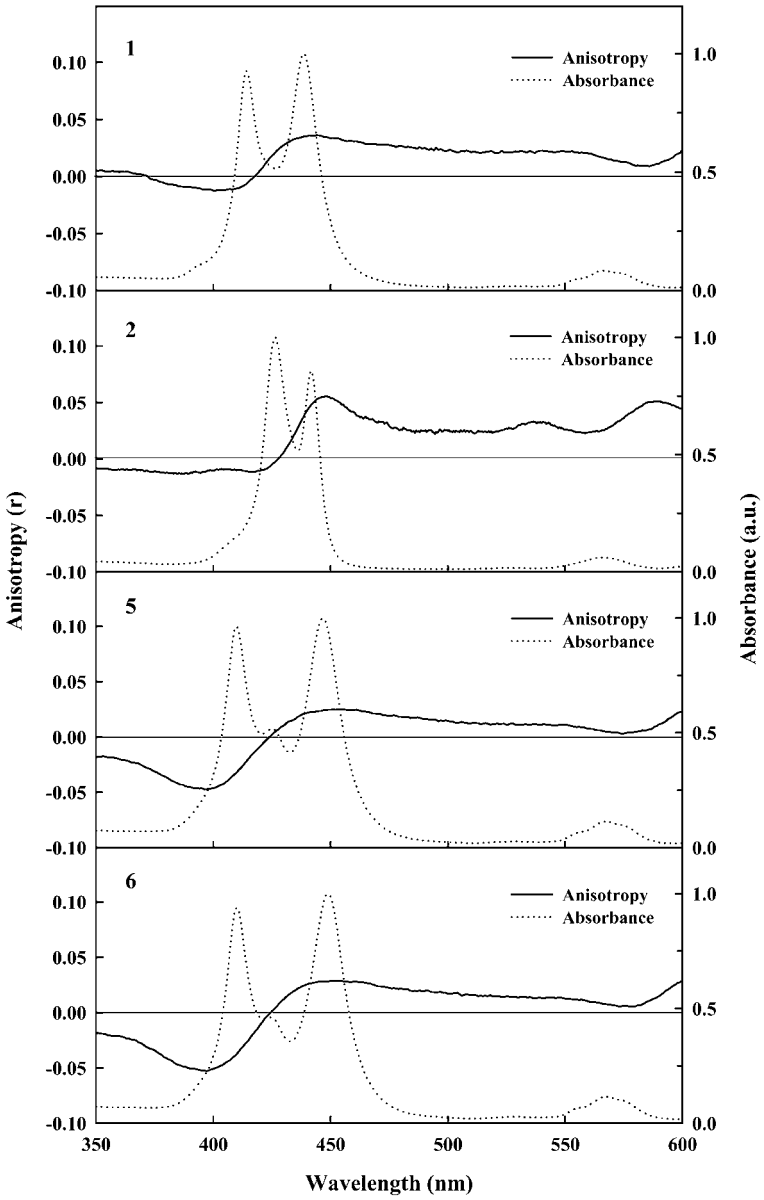

Figure 2. Steady-state fluorescence excitation anisotropy spectra of **1**, **2**, **5**, and **6** recorded in toluene, except for **2**, which was recorded in pyridine. The polarized excitation spectra (E_{VV} and E_{VH}) were measured at the emission wavelength 625 nm, and then the anisotropy spectra were calculated.

fluorescence anisotropy decay times are associated with the molecular volumes, indicating that the anisotropy decay originates from the molecular rotational diffusion motion in solution (see the Supporting Information). The fluorescence anisotropy decay time significantly increases in the formation of **5** and **6**, reflecting much increased molecular volumes relative to their constituent unit of **1**. In addition, complex **2** has a relatively slow rotational diffusion time in the strongly coordinating and viscous solvent pyridine. As listed in Table 2, the fluorescence anisotropy decays consistently revealing negative amplitudes, in agreement with the negative anisotropies in the high-energy Soret bands of the steady-state fluorescence excitation anisotropy spectra (Figure 2).

Femtosecond transient absorption and transient absorption anisotropy: To explore the fast excitation-energy migrations in **5** and **6**, both femtosecond transient absorption (TA), which includes pump-power dependence and transient absorption anisotropy (TAA) decays, were measured (Figures 4 and 5). The Q-band excitation, that is, $\lambda_{pump} =$ 575 nm, was employed to avoid an involvement of $S_2 \rightarrow S_1$ relaxation in the porphyrin. The TA and TAA decays of **1** and **2** were also measured as references (Figures 3 and 4a inset). It should be noted that **1** and **2** reveal no power dependence on the TA decay profile, with only slow decay components that are in agreement with the slow S_1 state lifetimes found in the TCSPC (time-correlated single-photon counting) measurements, that is, 2.33 and 1.82 ns for **1** and **2**, respectively (Table 3). In contrast, **1** and **2** show relatively fast anisotropy decay profiles in the time region of a few picoseconds, indicating fast depolarization channels, presumably due to the EEH between zinc(II)–porphyrin monomers (Figure 3). While the TAA decay of **1** shows only single decay component with a time constant of ~200 fs, that of **2** is fitted with two decay components, whereby the fast anisotropy decay component is similar to that of **1**. Because the B_x and B_y equilibrium process inside zinc(II)–porphyrin monomers proceeds on the timescale of ~200 fs,[21] the fast τ_1 component comes from both the dipole equilibrium of the zinc(II)–porphyrin monomer and the EEH between the zinc(II)–porphyrin monomers through the cofacial linkage of **1**, while the slow τ_2 component results from the EEH between zinc(II)–porphyrin monomers through the 1,3-phenylene linkage of **2**. Since the diporphyrin **2** does not have the cofacial unit, only the B_x and B_y equilibrium process contributes to the fast decay component. For comparison, the tetrameric porphyrin **3**, which has both the cofacial unit and the 1,3-phenylene linker, was measured (Figure 3, bottom). In this case, the decay curve can also be fitted with two components of 230 fs and 4.6 ps, which are almost the same as

Table 2. Fitted fluorescence lifetimes and anisotropy decay parameters of samples **1**, **2**, **5**, and **6**.[a]

	Fitted fluorescence lifetime[b] τ [ns][c]	Anisotropy decay parameters[d] r_0[e]	Φ [ns][e]
1	2.33±0.01 (100%)	−0.10±0.01	0.43±0.02
2	1.82±0.02 (100%)	−0.04±0.01	1.72±0.02
5	2.18±0.01 (100%)	−0.13±0.01	2.22±0.02
6	2.19±0.01 (100%)	−0.12±0.01	2.84±0.02

[a] The solvents used were pyridine for **2** and toluene for the others; the excitation wavelength, 410 nm, was applied to all experiments. [b] The fluorescence lifetimes of the samples were obtained by averaging the fitted single fluorescence lifetimes at several emission wavelengths. [c] Obtained from the relation $I(t)=A\exp(-t/\tau)$, in which $I(t)$ is the time-dependent fluorescence intensity, A the amplitude (noted in parentheses as the percentage), and τ the fitted fluorescence lifetime; the χ^2 values of the fittings were maintained as 1.0–1.3. [d] The fluorescence anisotropy decays were monitored at $\lambda_{em}=625$ nm. [e] Obtained from the relation $r(t)=r_0\exp(-t/\Phi)$, in which $r(t)$ is the time-dependent fluorescence anisotropy $[r(t)=(I_{\parallel}(t)-GI_{\perp}(t))/(I_{\parallel}(t)+2GI_{\perp}(t)]$, r_0 the initial anisotropy value, and Φ the fitted anisotropy decay time.

those of **2**. On the other hand, the r_{inf} value of 0.05 for **3** is smaller than that of 0.09 for **2**, indicating that the B_x–B_y equilibrium and the EEHs within and between units of **1** simultaneously occur in **3**. The details of measurement and analysis of **3** are described in the Supporting Information.

The TA decays of **5** and **6** are very sensitive to the pump power. When the pump power is increased, the contributions of relatively fast τ_1 and τ_2 components are enhanced, with respect to those of slowest τ_3 ones (Figures 4a, 5a, and Table 3). The pump-power dependence on the TA decay is a strong indication of S_1–S_1 exciton–exciton annihilation, because the intense excitation or high density of photons may generate two or more excitons in one cyclic array, then the recombination between the excitons gives rise to a fast deactivation channel.[22,23] Figures 4a and 5a indicate that the exciton–exciton annihilation of **5** and **6** is due to the exciton–exciton recombination between units of **1** rather than zinc(II)–porphyrin monomers, because this process does not occur in **1**. The exciton–exciton annihilation process implies a Förster-type energy transfer from the excited donor to the nearest excited acceptor, resulting in a doubly excited acceptor state, which then quickly relaxes to the singly excited state.[22,23]

Arrays **5** and **6** have relatively fast TAA decays in the time region of a few picoseconds, reflecting the fast depolarizations arising from the energy migration (Figures 4c and 5c). It is evident that the r_{inf} value of 0.22 in **1** decreases to 0.07 in **5** and further to 0.02 in **6**, reflecting additional depolarization channels[20] due to the energy migration along the entire cyclic arrays. In view of energy-hopping dynamics, the fast τ_1 TAA decay of **5** and **6** is due to the depolarization process inside units of **1**, because a similar time constant of ~200 fs was observed in **1**. On the other hand, the slow τ_2 components are responsible for the EEHs through the 1,3-phenylene linkages of **5** and **6**, because the similar time constant of 4.7 ps was observed in **2** (Figures 3, 4c, and 5c). It should be noted that there is a discrepancy between the

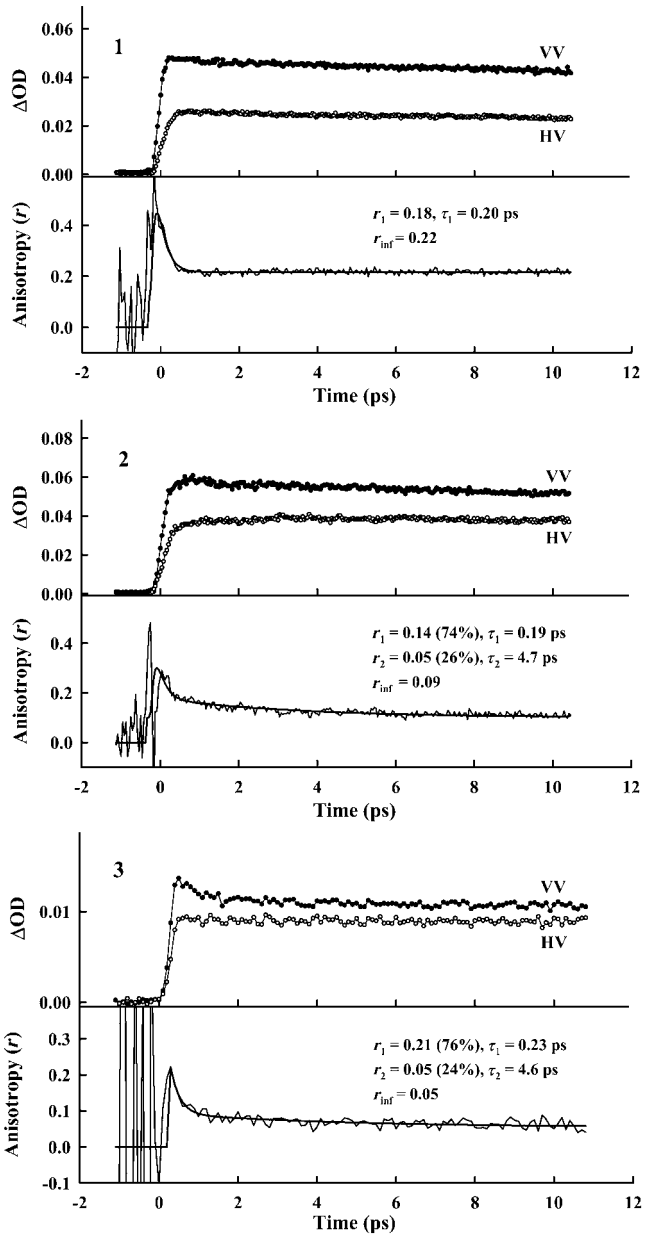

Figure 3. Transient absorption anisotropy decay profiles of **1** in toluene, **2** in pyridine, and **3** in dimethylformamide (DMF), in which the polarized transient absorption decays for parallel (VV) and perpendicular (HV) orientations between pump and probe beams are included in each panel. Insets show the deconvolution fitted anisotropy decay parameters with a train of 150 fs pump pulse. The pump and probe wavelengths are 575 and 490 nm, which are the Q-band pump and induced-absorption probe, respectively.

TAA decay times and the exciton–exciton annihilation times in both **5** and **6**. In multichromophore systems, however, neither exciton–exciton annihilation nor anisotropy depolarization time directly represents the EEH time between the energy-hopping sites, because they do not occur in a single donor–acceptor pair. The EEH time can only be calculated by simulating the EEH process by using these two observables simultaneously.

Table 3. Transient absorption decay parameters for samples **1**, **2**, **5**, and **6**.[a]

	Pump power [mW]	Fitted decay times [ps][b] τ_1	τ_2	τ_3
1	1.0	2330 (100%)		
	0.5	2330 (100%)		
	0.2	2330 (100%)		
2	1.0	1820 (100%)		
	0.5	1820 (100%)		
	0.2	1820 (100%)		
5	1.0	1.33 (23%)	8.30 (22%)	2180 (55%)
	0.5	1.15 (18%)	8.25 (20%)	2180 (62%)
	0.2	1.23 (12%)	8.25 (15%)	2180 (73%)
6	1.0	1.50 (29%)	8.30 (21%)	2190 (50%)
	0.5	1.50 (20%)	8.27 (17%)	2190 (63%)
	0.2	1.50 (20%)	8.27 (06%)	2190 (74%)

[a] The pump and probe wavelengths are 575 and 490 nm, and the solvents used were pyridine for **2** and toluene for the others. [b] Obtained from the relation $\Delta OD(t) = A_1\exp(-t/\tau_1) + A_2\exp(-t/\tau_2) + A_3\exp(-t/\tau_3)$, in which $\Delta OD(t)$ is the transient absorption intensity, A the amplitude (noted in parentheses as the normalized percentage, that is, $[A_i/(A_1+A_2+A_3)]\times 100$), and τ the fitted decay time.

Discussion

Excitonic dipole–dipole interaction: The absorption spectra of **5** and **6** can be qualitatively explained in terms of exciton coupling theory.[24] The Soret band of the porphyrin has two perpendicular transition dipole moments B_y and B_z that are degenerate. In the cofacial zinc(II)–diporpyrin **1**, two transition dipole moments B_y are coupled as a J-aggregate to give rise to the red-shifted Soret band, and B_z are coupled as an H-aggregate to give rise to the blue-shifted Soret band, respectively (Scheme 2, left). In addition, the Soret band is further split through the 1,3-phenylene linkage of **5** and **6**. The dipole moments of **5** and **6** consist of the dipole moments parallel (B_y) and perpendicular (B_z) to the long axis of the cyclic arrays. These dipole moments are coupled in a similar manner to that of **1**. For the B_y components, the in-phase arrangement of transition dipoles is attractive and leads to a lowering of energy, and the out-of-phase arrangement of transition dipoles is repulsive and causes an increase in energy (Scheme 2, right). In contrast, for the B_z components, the in-phase arrangement of transition dipoles is repulsive and leads to an increase in energy, whereas the dipole–dipole interaction between out-of-phase arrangements should be cancelled (Scheme 2, right). The Soret band splitting of **6** is larger than that of **5** by 100 cm^{-1}, indicating that the exciton interaction in **6** is slightly larger than that in **5**.

EEH time through 1,3-phenylene linkage of 2 and 3: The EEH process of **2** and **3** is reversible between porphyrin units, which is conceived as a simple equilibrium as shown in Equation (1) in which P represents the porphyrin unit, k_1

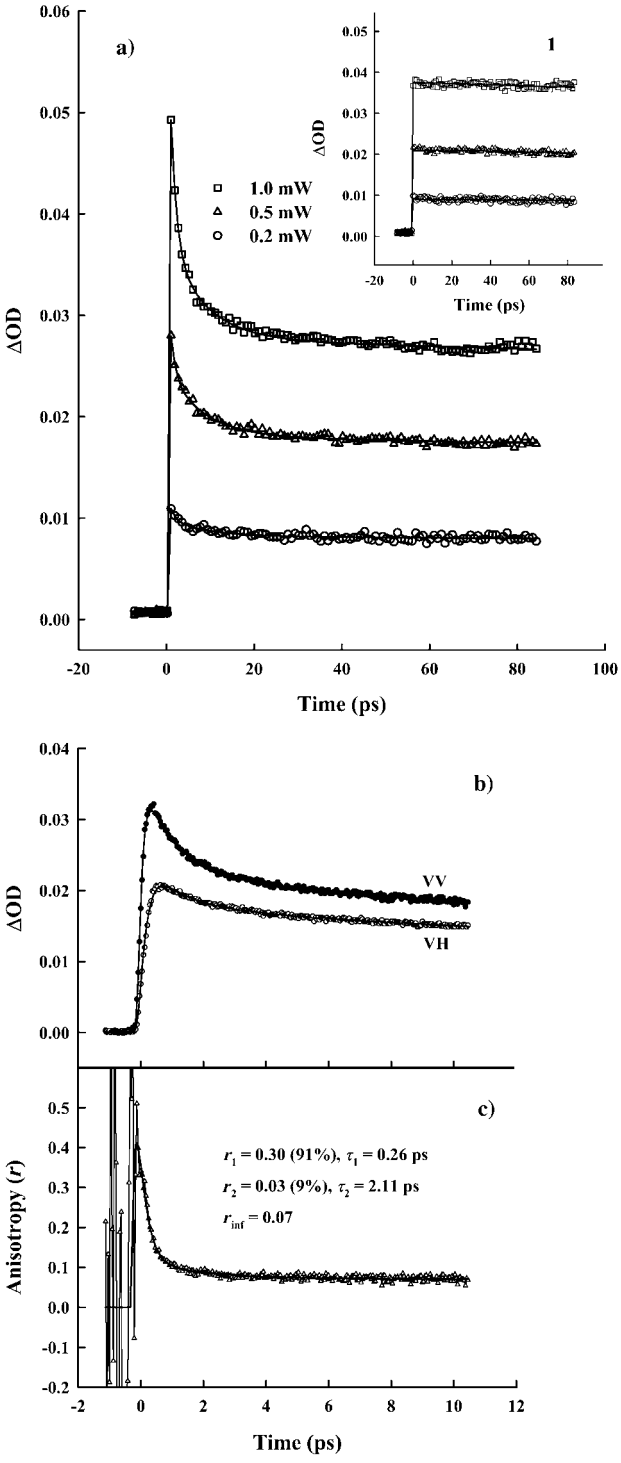

Figure 4. a) Transient absorption decay profiles of **5**, which include pump power dependence, whereby the pump and probe wavelengths are 575 and 490 nm, that is, the Q-band pump and induced-absorption probe (inset shows the transient absorption decay profiles of **1** that include pump power dependence). b) Polarized transient absorption decays of **5** for parallel (VV) and perpendicular (VH) orientations between pump and probe beams. c) Transient absorption anisotropy decay profiles of **5**, for which the pump and probe wavelengths are 575 and 490 nm; the inset shows the deconvolution fitted anisotropy decay parameters. The solvent used was toluene.

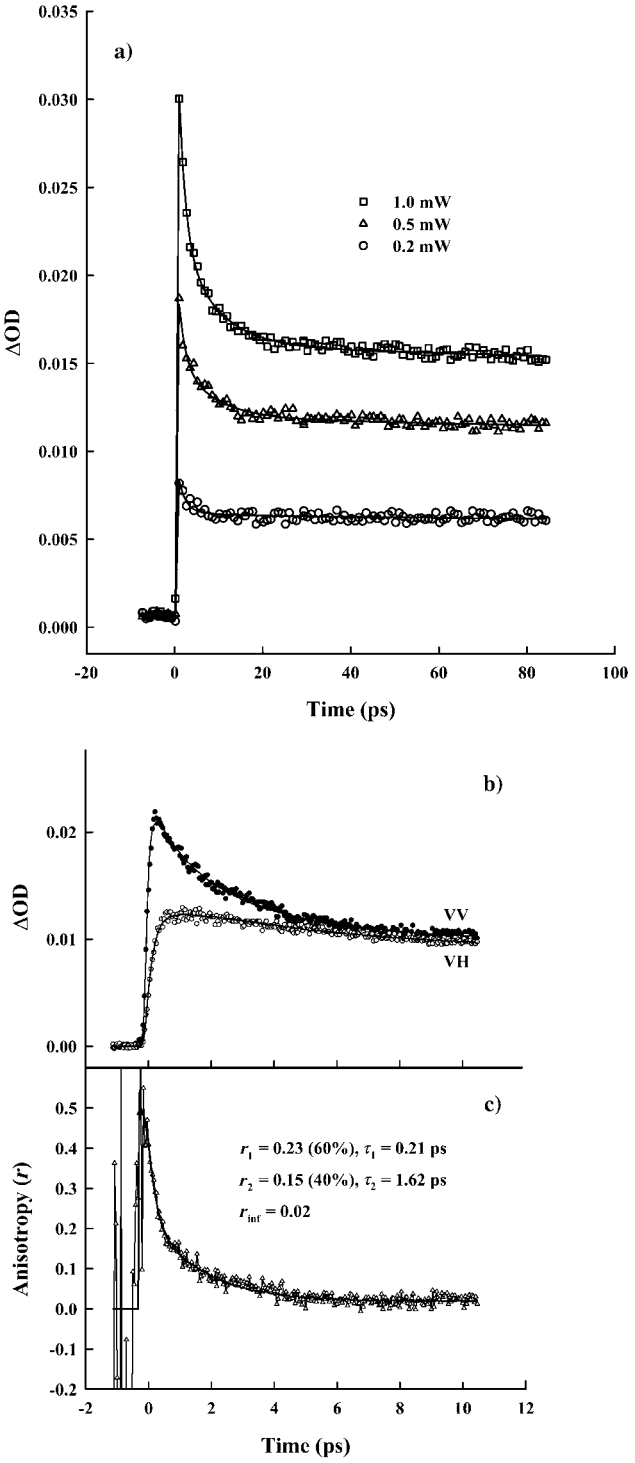

Figure 5. a) Transient absorption decay profiles of **6** that include pump power dependence, for which the pump and probe wavelengths are 575 and 490 nm, that is, the Q-band pump and induced-absorption probe. b) Polarized transient absorption decays of **6** for parallel (VV) and perpendicular (VH) orientations between pump and probe beams. c) Transient absorption anisotropy decay profiles of **6**, for which the pump and probe wavelengths are 575 and 490 nm; the inset shows the deconvolution fitted anisotropy decay parameters. The solvent used was toluene.

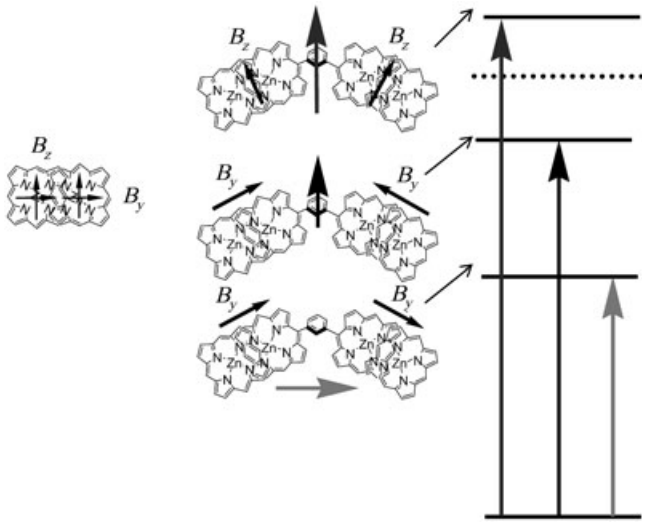

Scheme 2. Excitonic dipole–dipole coupling within **5** and **6**.

and k_{-1} are forward and reverse reaction rate constants, respectively, which correspond to the EEH times.

$$P^* + P \underset{k_{-1}}{\overset{k_1}{\rightleftharpoons}} P + P^* \quad (1)$$

Because the EEH time through the 1,3-phenylene linkage corresponds to the slow τ_2 TAA decay component, the relaxation time of the above Scheme can be defined by Equation (2)

$$\tau_2 = \frac{1}{k_1 + k_{-1}} \quad (2)$$

From Equation (2), the EEH rate constants through the 1,3-phenylene linkage are determined as $1.06\times10^{11}\ s^{-1}$ ($(9.4\ ps)^{-1}$) with $\tau_2 = 4.7$ ps for **2** and $1.09\times10^{11}\ s^{-1}$ ($(9.2\ ps)^{-1}$) with $\tau_2 = 4.6$ ps for **3**.

Excitation-energy migration within 5 and 6: We have examined the EEH processes of **5** and **6** by using the exciton–exciton annihilation and anisotropy depolarization. When Förster-type energy-transfer model is employed by assuming a migration-limited character of exciton–exciton annihilation and a random-walk formalism of anisotropy decay, the EEH time can be deduced from the analytical depolarization and exciton–exciton annihilation times through Equations (3) and (4) in which N is the number of excitation energy hopping sites, α is the angle between the neighboring transition dipoles, $\tau_{annihilation}$ is the slowest exciton–exciton annihilation time, and $\tau_{hopping}$ is the inverse of the nearest neighbor energy-hopping rate.[22]

$$\tau_{depolarization} = \frac{\tau_{hopping}}{4(1-\cos^2(2\pi/N))} = \frac{\tau_{hopping}}{4(1-\cos^2\alpha)} \quad (3)$$

$$\tau_{annihilation} = \frac{N^2-1}{24}\,\tau_{hopping} \quad (4)$$

Equation (3) is understood by considering that the depolarization is complete when the transition dipole migrates through 90° and how many hops are required for one cycle of this rotation. On the other hand, Equation (4) assumes that the exciton–exciton annihilation reflects the migration-limited exciton–exciton recombination process along the cyclic array and how many hops are required for this recombination to be accomplished.

The EEH times within **5** and **6** are calculated by using the exciton–exciton annihilation and anisotropy decay times, given in Table 3 and Figures 4 and 5. Because arrays **5** and **6** consist of five and six cofacial zinc(II)–diporphyrin units of **1**, the numbers of hopping sites should be $N=5$ and 6, respectively. Introducing $N=5$ and $\alpha=72°$ to Equations (3) and (4) results in the $\tau_{hopping}=3.62\times\tau_{depolarization}$ and $\tau_{hopping}=\tau_{annihilation}$ for **5**.[22] Similarly, introducing $N=6$ and $\alpha=60°$ leads to $\tau_{hopping}=3.00\times\tau_{depolarization}$ and $\tau_{hopping}=0.686\times\tau_{annihilation}$ for **6**.[22] As consequence, the EEH times between the adjacent cofacial zinc(II)–diporphyrin units through the 1,3-phenylene linkage are calculated to be 7.6 ps for **5** and 4.9 ps for **6** with the anisotropy decay times of 2.11 and 1.62 ps, given in Figures 4c and 5c, respectively. In a different approach, by using the slowest exciton–exciton annihilation decay times of ~8.3 ps for **5** and **6**, as given in Table 3, the EEH times were evaluated to be 8.3 ps for **5** and 5.7 ps for **6**. It is worth noting that the two different experimental observables, exciton–exciton annihilation and anisotropy depolarization, result in consistent EEH times (8.0 ± 0.5 ps and 5.3 ± 0.6 ps) within small error ranges. The excitation-energy migration process, thus, is well described by the Förster-type incoherent energy-hopping model, assuming the well-arranged cyclic systems of **5** and **6**.

Interesting is that **5** and **6** have faster EEH times (8.0 and 5.3 ps) than the ~9 ps of linear porphyrin arrays **2** and **3**, and that **6** has a faster EEH time than **5**. The accelerated hopping rate in the cyclic porphyrin arrays is rationalized in terms of a rigid geometry of **5** and **6**, in which the well-arranged and fixed porphyrin units have an advantage in dipole–dipole resonance with respect to the porphyrin units in random motion in the linear complexes **2** and **3**. The accelerated hopping rate of **6** relative to that of **5** can be accounted for in terms of different dipole coupling strength between cofacial zinc(II)–diporphyrin units observed as a larger splitting of the Soret band of **6** (2119 cm^{-1}) than that of **5** (2019 cm^{-1}). Another possible consideration is the transient orientation or fluctuation caused by twist (or rotational) motions of units of **1** with respect to the *m*-phenylene group. Adjacent units of **1** may twist in the opposite direction to each other, whereby the *meso*-substituted phenylene groups in the encountering positions twist against the porphyrin plane in reverse direction. In the case of **6**, which has an even number of units of **1**, alternating disrotatory motion between adjacent units allows closer approaches to coplanar orientation over the molecule to facilitate the delocalization of excitation and the energy transfer rate of **6**. In contrast, array **5**, with an odd number of units of **1**, does not permit the coplanar conformation over the molecule and the delocalization may be limited within dimer, leading to the relatively slow energy-transfer rate similar to **2** and **3**. It would be interesting to consider such a difference in even–odd number of constituent units in future studies as a working hypothesis.

Conclusion

We have investigated the excitation-energy migration process within two dimensional cyclic porphyrin arrays **5** and **6**, which have been prepared by the intermolecular coordination and ring-closing metathesis reactions of *meso*-olefinic substituents. Both exciton–exciton annihilation and anisotropy depolarization describe well the energy migration process among the cofacially linked zinc(II)–diporphyrin units of **1** in **5** and **6**. Assuming the number of energy-hopping sites is $N=5$ and 6, the two different experimental observables consistently give the EEH times of 8.0 ± 0.5 and 5.3 ± 0.6 ps through the 1,3-phenylene linkages of **5** and **6**, respectively. The obtained EEH times of **5** and **6** are faster than those of the linear porphyrin arrays **2** or **3**, because of a well-arranged and fixed circular geometry of the pigments. The faster EEH time of **6** relative to that of **5** is rationalized by considering the different dipole–dipole coupling strength as observed in the steady-state absorption spectra, as well as the differences in transient orientation between **5** and **6** arising from the even and odd number of cofacial diporphyrin units in **5** and **6**. Overall, the investigation on the excitation-energy migration process of **5** and **6** affords a well-defined molecular model for the complicated excitation-energy migration process occurring in natural light-harvesting systems.

Experimental Section

Steady-state spectra: The samples were prepared in approximately micromolar concentrations in toluene or pyridine. All the solvents (~99.9% purity) were purchased from Merck Chemical Co. (HPLC grade). Absorption spectra were obtained with a Shimadzu model 1601 UV spectrometer, and steady-state fluorescence and fluorescence excitation spectra were measured by a Hitachi model F-4500 fluorescence spectrophotometer at room temperature. Steady-state fluorescence excitation anisotropy spectra were obtained by changing the fluorescence detection polarization either parallel or perpendicular to the polarization of the excitation light. The excitation anisotropy spectra then were calculated by using Equation (5) in which E_{VV} (or E_{VH}) is the fluorescence excitation spectrum when the excitation light is vertically polarized and only the vertically (or horizontally) polarized portion of fluorescence is detected, that is, the first and second subscripts represent excitation and detection polarization, respectively. The factor G is defined by I_{VV}/I_{VH}, which is equal to the ratio of the sensitivities of the detection system for vertically and horizontally polarized light.

$$r=\frac{E_{VV}-GE_{VH}}{E_{VV}+2GE_{VH}} \tag{5}$$

Time-resolved fluorescence decay: A picosecond time-resolved time-correlated single-photon-counting system was used for the fluorescence decay and fluorescence anisotropy decay measurements. The system has been described in previous reports.[6g,9b,19]

Femtosecond TA and TAA decay: A dual-beam femtosecond time-resolved transient absorption spectrometer that included an IR-OPA (infrared optical parametric amplification) pump and white light continuum probe was employed for TA and TAA measurements. The system has also been described in previous reports.[6g,9b,19]

Acknowledgements

This research was financially supported by the National Creative Research Initiatives Program of the Korea Science and Engineering Foundation of Korea (D.K.). The work at Osaka was partly supported by a Grant-in-Aid for Scientific Research on Priority Areas (432) from the Ministry of Education, Culture, Sports, Science, and Technology (MEXT) of the Japanese Government (H.M.). The work at Nara was supported by CREST (Core Research for Evolutional Science and Technology) of Japan Science and Technology Corp. (JST) and by Grant-in-Aids for Scientific Research (A) (No. 15205020), for Scientific Research on Priority Areas (No. 15036248, Reaction Control of Dynamic Complexes) from the Ministry of Education, Culture, Sports, Science and Technology, Japan (Monbu Kagakusho) (Y.K.).

[1] M. R. Wasielewski, *Chem. Rev.* **1992**, *92*, 435.
[2] D. Gust, T. A. Moore, A. L. Moore, *Acc. Chem. Res.* **2001**, *34*, 40.
[3] D. Holten, D. F. Bocian, J. S. Lindsey, *Acc. Chem. Res.* **2002**, *35*, 57.
[4] M. P. Debreczeny, W. A. Svec, E. M. Marsh, M. R. Wasielewski, *J. Am. Chem. Soc.* **1996**, *118*, 8174.
[5] G. Kodis, P. A. Liddell, L. de la Garza, P. C. Clausen, J. S. Lindsey, A. L. Moore, T. A. Moore, D. Gust, *J. Phys. Chem. A* **2002**, *106*, 2036.
[6] a) D. Kim, A. Osuka, *J. Phys. Chem. A* **2003**, *107*, 8791; b) A. Tsuda, A. Osuka, *Science* **2001**, *293*, 79; c) H. S. Cho, D. H. Jeong, S. Cho, D. Kim, Y. Matsuzaki, K. Tanaka, A. Tsuda, A. Osuka, *J. Am. Chem. Soc.* **2002**, *124*, 14642; d) N. Aratani, H. S. Cho, T. K. Ahn, S. Cho, D. Kim, H. Sumi, A. Osuka, *J. Am. Chem. Soc.* **2003**, *125*, 9668; e) H. S. Cho, H. Rhee, J. K. Song, C.-K. Min, M. Takase, N. Aratani, S. Cho, A. Osuka, T. Joo, D. Kim, *J. Am. Chem. Soc.* **2003**, *125*, 5849; f) X. Peng, N. Aratani, A. Takagi, T. Matsumoto, T. Kawai, I.-W. Hwang, T. K. Ahn, D. Kim, A. Osuka, *J. Am. Chem. Soc.* **2004**, *126*, 4468; g) Y. Nakamura, I.-W. Hwang, N. Aratani, T. K. Ahn, D. M. Ko, A. Takagi, T. Kawai, T. Matsumoto, D. Kim, A. Osuka, *J. Am. Chem. Soc.* **2005**, *127*, 236.
[7] a) M.-S. Choi, T. Yamazaki, I. Yamazaki, T. Aida, *Angew. Chem.* **2004**, *116*, 152; *Angew. Chem. Int. Ed.* **2004**, *43*, 150; b) M.-S. Choi, T. Aida, T. Yamazaki, I. Yamazaki, *Chem. Eur. J.* **2002**, *8*, 2667; c) M.-S. Choi, T. Aida, H. Luo, Y. Araki, O. Ito, *Angew. Chem.* **2003**, *115*, 4194; *Angew. Chem. Int. Ed.* **2003**, *42*, 4060.
[8] a) D. L. Officer, A. K. Burrell, D. C. W. Reid, *Chem. Commun.* **1996**, 1657; b) C. C. Mak, N. Bampos, J. K. M. Sanders, *Angew. Chem.* **1998**, *110*, 3169; *Angew. Chem. Int. Ed.* **1998**, *37*, 3020; c) N. Solladie, M. Gross, J.-P. Gisselbrecht, C. Sooambar, *Chem. Commun.* **2001**, 2206; d) H. A. M. Biemans, A. E. Rowan, A. Verhoeven, P. Vanoppen, L. Latterini, J. Foekema, A. P. H. J. Schenning, E. W. Meijer, F. C. de Schryver, R. J. M. Nolte, *J. Am. Chem. Soc.* **1998**, *120*, 11054; e) S. Rucareanu, O. Mongin, A. Schuwey, N. Hoyler, A. Gossauer, W. Amrein, H.-U. Hediger, *J. Org. Chem.* **2001**, *66*, 4973; f) E. K. L. Yeow, K. P. Ghiggino, J. N. H. Reek, M. J. Crossley, A. W. Bosman, A. P. H. J. Schenning, E. W. Meijer, *J. Phys. Chem. B* **2000**, *104*, 2596; g) P. L. Taylor, A. P. Wylie, J. Huuskonen, H. L. Anderson, *Angew. Chem.* **1998**, *110*, 1033; *Angew. Chem. Int. Ed.* **1998**, *37*, 986.
[9] a) A. Tsuda, T. Nakamura, S. Sakamoto, K. Yamaguchi, A. Osuka, *Angew. Chem.* **2002**, *114*, 2941; *Angew. Chem. Int. Ed.* **2002**, *41*, 2817; b) I.-W. Hwang, H. S. Cho, D. H. Jeong, D. Kim, A. Tsuda, T. Nakamura, A. Osuka, *J. Phys. Chem. B* **2003**, *107*, 9977; c) I.-W. Hwang, T. Kamada, T. K. Ahn, D. M. Ko, T. Nakamura, A. Tsuda, A. Osuka, D. Kim, *J. Am. Chem. Soc.* **2004**, *126*, 16187.
[10] a) K. Ogawa, Y. Kobuke, *Angew. Chem.* **2000**, *112*, 4236; *Angew. Chem. Int. Ed.* **2000**, *39*, 4070; b) K. Ogawa, T. Zhang, K. Yoshihara, Y. Kobuke, *J. Am. Chem. Soc.* **2002**, *124*, 22; c) Y. Kobuke, K. Ogawa, *Bull. Chem. Soc. Jpn.* **2003**, *76*, 689; d) R. Takahashi, Y. Kobuke, *J. Am. Chem. Soc.* **2003**, *125*, 2372; e) Y. Kuramochi, A. Satake, Y. Kobuke, *J. Am. Chem. Soc.* **2004**, *126*, 8668.
[11] a) J.-M. Lehn, *Science* **2002**, *295*, 2400; b) M. D. Hollingsworth, *Science* **2002**, *295*, 2410.
[12] a) T. Hayashi, H. Ogoshi, *Chem. Soc. Rev.* **1997**, *26*, 355; b) T. Imamura, K. Fukushima, *Coord. Chem. Rev.* **2000**, *198*, 133; c) J. Wojaczynski, L. Latos-Grazynski, *Coord. Chem. Rev.* **2000**, *204*, 113; d) A. V. Chernook, U. Rempel, C. van Borczyskowski, A. M. Shulga, E. I. Zenkevich, *Chem. Phys. Lett.* **1996**, *254*, 229; e) L. Flamigni, M. R. Johnson, *New J. Chem.* **2001**, *25*, 1368; f) R. D. Hartnell, D. P. Arnold, *Organomet. Chem.* **2004**, *23*, 391.
[13] a) C. A. Hunter, J. K. M. Sanders, G. S. Beddard, S. Evans, *J. Chem. Soc. Chem. Commun.* **1989**, 1765; b) S. Anderson, H. L. Anderson, J. K. M. Sanders *Acc. Chem. Res.* **1993**, *26*, 469.
[14] a) G. S. Wilson, H. L. Anderson, *Chem. Commun.* **1999**, 1539; b) P. N. Taylor, H. L. Anderson, *J. Am. Chem. Soc.* **1999**, *121*, 11538; c) T. E. Screen, J. R. G. Thorne, R. G. Denning, D. G. Bucknall, H. L. Anderson, *J. Am. Chem. Soc.* **2002**, *124*, 9712; d) T. E. Screen, J. R. G. Thorne, R. G. Denning, D. G. Bucknall, A H. L. nderson, *J. Mater. Chem.* **2003**, *13*, 2796.
[15] a) C. A. Hunter, R. K. Hyde, *Angew. Chem.* **1996**, *108*, 2064; *Angew. Chem. Int. Ed. Engl.* **1996**, *35*, 1936; b) R. A. Haycock, A. Yartsev, U. Michelsen, V. Sundström, C. A. Hunter, *Angew. Chem.* **2000**, *112*, 3762; *Angew. Chem. Int. Ed.* **2000**, *39*, 3616.
[16] C. Jungas, J. Ranck, J. Rigaud, P. Joliot, A. Vermeglio, *EMBO J.* **1999**, *18*, 534.
[17] C. Ikeda, A. Satake, Y. Kobuke, *Org. Lett.* **2003**, *5*, 4935.
[18] U. Ermler, G. Fritzsch, S. Buchanan, H. Michel, *Structure* **1994**, *2*, 925.
[19] a) Y. H. Kim, D. H. Jeong, D. Kim, S. C. Jeoung, H. S. Cho, S. K. Kim, N. Aratani, A. Osuka, *J. Am. Chem. Soc.* **2001**, *123*, 76; b) H. S. Cho, N. W. Song, Y. H. Kim, S. C. Jeoung, S. Hahn, D. Kim, S. K. Kim, N. Yoshida, A. Osuka, *J. Phys. Chem. A* **2000**, *104*, 3287.
[20] A. Morandeira, E. Vauthey, A. Schuwey, A. Gossauer, *J. Phys. Chem. A* **2004**, *108*, 5741.
[21] C. Galli, K. Wynne, S. M. LeCours, M. J. Therien, R. M. Hochstrasser, *Chem. Phys. Lett.* **1993**, *206*, 493.
[22] S. E. Bradforth, R. Jimenez, F. van Mourik, R. van Grondelle, G. R. Fleming, *J. Phys. Chem.* **1995**, *99*, 16179.
[23] a) G. Trinkunas, J. L. Herek, T. Polívka, V. Sundström, T. Pullerits, *Phys. Rev. Lett.* **2001**, *86*, 4167; b) G. Trinkunas, *J. Lumin.* **2003**, *102*, 532; c) B. Brüggemann, V. May, *J. Chem. Phys.* **2004**, *120*, 2325; d) M. G. Müller, M. Hucke, M. Reus, A. R. Holzwarth, *J. Phys. Chem.* **1996**, *100*, 9537; e) B. Brüggemann, J. L. Herek, V. Sundström, T. Pullerits, V. May, *J. Phys. Chem. B* **2001**, *105*, 11391.
[24] a) M. Kasha, *Radiat. Res.* **1963**, *20*, 55; b) M. Kasha, H. R. Rawls, M. A. El-Bayoumi, *Pure Appl. Chem.* **1965**, *11*, 371; c) G. D. Scholes, K. P. Ghiggino, *J. Phys. Chem.* **1994**, *98*, 4580.

Received: January 19, 2005
Published online: April 13, 2005

